unfavorable[31] and patients who may be rendered transplantable after hepatectomy may be selected. However, microscopic portal invasion cannot be diagnosed preoperatively and a pathological examination is required to evaluate this factor. From our current data, the AP-factor was shown to be very closely related to both tumor differentiation and vascular invasion and was selected as an independent factor related to survival with an equal *P*-value to microscopic portal invasion, and an independent factor related to recurrence with a lower *P*-value. Hence, the AP-factor is suggested to be a critical HCC marker with an accuracy that equals microscopic portal invasion at preoperatively predicting tumor malignancy. Hence, HCC patients in whom the same outcomes can be expected for hepatectomy as with transplantation or who may be rendered transplantable by hepatectomy could be selected by measuring their AP-factor.

REFERENCES

1 Arii S, Yamaoka Y, Futagawa S *et al.* Results of surgical and nonsurgical treatment for small-sized hepatocellular carcinomas: a retrospective and nationwide survey in Japan. The Liver Cancer Study Group of Japan. *Hepatology* 2000; **32** (6): 1224–9.

2 Kamiyama T, Nakanishi K, Yokoo H *et al.* Recurrence patterns after hepatectomy of hepatocellular carcinoma: implication of Milan criteria utilization. *Ann Surg Oncol* 2009; **16** (6): 1560–71.

3 Ikai I, Arii S, Kojiro M *et al.* Reevaluation of prognostic factors for survival after liver resection in patients with hepatocellular carcinoma in a Japanese nationwide survey. *Cancer* 2004; **101** (4): 796–802.

4 Sasaki Y, Yamada T, Tanaka H *et al.* Risk of recurrence in a long-term follow-up after surgery in 417 patients with hepatitis B- or hepatitis C-related hepatocellular carcinoma. *Ann Surg* 2006; **244** (5): 771–80.

5 Jonas S, Bechstein WO, Steinmuller T *et al.* Vascular invasion and histopathologic grading determine outcome after liver transplantation for hepatocellular carcinoma in cirrhosis. *Hepatology* 2001; **33** (5): 1080–6.

6 Shirabe K, Itoh S, Yoshizumi T *et al.* The predictors of microvascular invasion in candidates for liver transplantation with hepatocellular carcinoma-with special reference to the serum levels of des-gamma-carboxy prothrombin. *J Surg Oncol* 2007; **95** (3): 235–40.

7 Shimada M, Takenaka K, Fujiwara Y *et al.* Des-gamma-carboxy prothrombin and alpha-fetoprotein positive status as a new prognostic indicator after hepatic resection for hepatocellular carcinoma. *Cancer* 1996; **78** (10): 2094–100.

8 Tamura S, Kato T, Berho M *et al.* Impact of histological grade of hepatocellular carcinoma on the outcome of liver transplantation. *Arch Surg* 2001; **136** (1): 25–30.

9 Toyoda H, Kumada T, Kiriyama S *et al.* Prognostic significance of simultaneous measurement of three tumor markers in patients with hepatocellular carcinoma. *Clin Gastroenterol Hepatol* 2006; **4** (1): 111–7.

10 Imamura H, Matsuyama Y, Tanaka E *et al.* Risk factors contributing to early and late phase intrahepatic recurrence of hepatocellular carcinoma after hepatectomy. *J Hepatol* 2003; **38** (2): 200–7.

11 Izumi R, Shimizu K, Ii T *et al.* Prognostic factors of hepatocellular carcinoma in patients undergoing hepatic resection. *Gastroenterology* 1994; **106** (3): 720–7.

12 Kondo K, Chijiiwa K, Makino I *et al.* Risk factors for early death after liver resection in patients with solitary hepatocellular carcinoma. *J Hepatobiliary Pancreat Surg* 2005; **12** (5): 399–404.

13 Shirabe K, Kanematsu T, Matsumata T, Adachi E, Akazawa K, Sugimachi K. Factors linked to early recurrence of small hepatocellular carcinoma after hepatectomy: univariate and multivariate analyses. *Hepatology* 1991; **14** (5): 802–5.

14 Nomura F, Ohnishi K, Tanabe Y. Clinical features and prognosis of hepatocellular carcinoma with reference to serum alpha-fetoprotein levels. Analysis of 606 patients. *Cancer* 1989; **64** (8): 1700–7.

15 Hanazaki K, Kajikawa S, Koide N, Adachi W, Amano J. Prognostic factors after hepatic resection for hepatocellular carcinoma with hepatitis C viral infection: univariate and multivariate analysis. *Am J Gastroenterol* 2001; **96** (4): 1243–50.

16 Matsumoto Y, Suzuki T, Asada I, Ozawa K, Tobe T, Honjo I. Clinical classification of hepatoma in Japan according to serial changes in serum alpha-fetoprotein levels. *Cancer* 1982; **49** (2): 354–60.

17 Mizejewski GJ. Alpha-fetoprotein structure and function: relevance to isoforms, epitopes, and conformational variants. *Exp Biol Med (Maywood)* 2001; **226** (5): 377–408.

18 Silver HK, Gold P, Shuster J, Javitt NB, Freedman SO, Finlayson ND. Alpha(1)-fetoprotein in chronic liver disease. *N Engl J Med* 1974; **291** (10): 506–8.

19 Fujiyama S, Tanaka M, Maeda S, Ashihara H, Hirata R, Tomita K. Tumor markers in early diagnosis, follow-up and management of patients with hepatocellular carcinoma. *Oncology* 2002; **62** (Suppl 1): 57–63.

20 Kasahara A, Hayashi N, Fusamoto H *et al.* Clinical evaluation of plasma des-gamma-carboxy prothrombin as a marker protein of hepatocellular carcinoma in patients with tumors of various sizes. *Dig Dis Sci* 1993; **38** (12): 2170–6.

21 Ikoma J, Kaito M, Ishihara T *et al.* Early diagnosis of hepatocellular carcinoma using a sensitive assay for serum des-gamma-carboxy prothrombin: a prospective study. *Hepatogastroenterology* 2002; **49** (43): 235–8.

© 2014 The Japan Society of Hepatology

22 Mita Y, Aoyagi Y, Yanagi M, Suda T, Suzuki Y, Asakura H. The usefulness of determining des-gamma-carboxy prothrombin by sensitive enzyme immunoassay in the early diagnosis of patients with hepatocellular carcinoma. *Cancer* 1998; **82** (9): 1643–8.
23 Inoue S, Nakao A, Harada A, Nonami T, Takagi H. Clinical significance of abnormal prothrombin (DCP) in relation to postoperative survival and prognosis in patients with hepatocellular carcinoma. *Am J Gastroenterol* 1994; **89** (12): 2222–6.
24 Koike Y, Shiratori Y, Sato S *et al.* Des-gamma-carboxy prothrombin as a useful predisposing factor for the development of portal venous invasion in patients with hepatocellular carcinoma: a prospective analysis of 227 patients. *Cancer* 2001; **91** (3): 561–9.
25 Sumie S, Kuromatsu R, Okuda K *et al.* Microvascular invasion in patients with hepatocellular carcinoma and its predictable clinicopathological factors. *Ann Surg Oncol* 2008; **15** (5): 1375–82.
26 Kaibori M, Matsui Y, Yanagida H, Yokoigawa N, Kwon AH, Kamiyama Y. Positive status of alpha-fetoprotein and des-gamma-carboxy prothrombin: important prognostic factor for recurrent hepatocellular carcinoma. *World J Surg* 2004; **28** (7): 702–7.
27 Kiriyama S, Uchiyama K, Ueno M *et al.* Triple positive tumor markers for hepatocellular carcinoma are useful predictors of poor survival. *Ann Surg* 2011; **254** (6): 984–91.
28 Figueras J, Jaurrieta E, Valls C *et al.* Resection or transplantation for hepatocellular carcinoma in cirrhotic patients: outcomes based on indicated treatment strategy. *J Am Coll Surg* 2000; **190** (5): 580–7.
29 Otto G, Heuschen U, Hofmann WJ, Krumm G, Hinz U, Herfarth C. Survival and recurrence after liver transplantation versus liver resection for hepatocellular carcinoma: a retrospective analysis. *Ann Surg* 1998; **227** (3): 424–32.
30 Poon RT, Fan ST, Lo CM, Liu CL, Wong J. Difference in tumor invasiveness in cirrhotic patients with hepatocellular carcinoma fulfilling the Milan criteria treated by resection and transplantation: impact on long-term survival. *Ann Surg* 2007; **245** (1): 51–8.
31 Shimoda M, Ghobrial RM, Carmody IC *et al.* Predictors of survival after liver transplantation for hepatocellular carcinoma associated with Hepatitis C. *Liver Transpl* 2004; **10** (12): 1478–86.

© 2014 The Japan Society of Hepatology

Carcinogenesis vol.35 no.2 pp.272–281, 2014
doi:10.1093/carcin/bgt343
Advance Access publication October 15, 2013

Heat shock factor 1 accelerates hepatocellular carcinoma development by activating nuclear factor-κB/mitogen-activated protein kinase

Makoto Chuma*, Naoya Sakamoto, Akira Nakai[1], Shuhei Hige, Mitsuru Nakanishi, Mitsuteru Natsuizaka, Goki Suda, Takuya Sho, Kanako Hatanaka[2], Yoshihiro Matsuno[2], Hideki Yokoo[3], Toshiya Kamiyama[3], Akinobu Taketomi[3], Gen Fujii[4], Kosuke Tashiro[5], Yoko Hikiba[6], Mitsuaki Fujimoto[1], Masahiro Asaka and Shin Maeda[7]

Department of Gastroenterology and Hepatology, Hokkaido University, Kita 15, Nishi 7, Kita-ku, Sapporo 060-8638, Japan, [1]Department of Biochemistry and Molecular Biology, Yamaguchi University, Ube, Japan, [2]Department of Pathology and [3]Department of Gastroenterological Surgery I, Hokkaido University, Kita 15, Nishi 7, Kita-ku, Sapporo 060-8638, Japan, [4]Division of Cancer Prevention, National Cancer Center Research Institute, Tokyo, Japan, [5]Graduate School of Genetic Resources Technology, Kyushu University, Fukuoka, Japan, [6]Division of Gastroenterology, Institute for Adult Diseases, Asahi Life Foundation, Tokyo, Japan and [7]Department of Gastroenterology, Yokohama City University, Yokohama, Japan

*To whom correspondence should be addressed. Tel: +81 11-716-1611; Fax: +81 11-706-7867;
Email: mchuuma@med.hokudai.ac.jp

Heat shock factor 1 (HSF1), a major transactivator of stress responses, has been implicated in carcinogenesis in various organs. However, little is known about the biological functions of HSF1 in the development of hepatocellular carcinoma (HCC). To clarify the functional role of HSF1 in HCC, we established HSF1-knockdown (HSF1 KD) KYN2 HCC cells by stably expressing either small hairpin RNA (shRNA) against HSF1 (i.e. HSF1 KD) or control shRNA (HSF1 control). Tumorigenicity was significantly reduced in orthotopic mice with HSF1 KD cells compared with those with HSF1 control cells. Reduced tumorigenesis in HSF1 KD cells appeared attributable to increased apoptosis and decreased proliferation. Tumor necrosis factor-α-induced apoptosis was increased in HSF1 KD cells and HSF1$^{-/-}$ mouse hepatocytes compared with controls. Decreased expression of IκB kinase γ, a positive regulator of nuclear factor-κB, was also observed in HSF1 KD cells and HSF1$^{-/-}$ mouse hepatocytes. Furthermore, expression of bcl-2-associated athanogene domain 3 (BAG3) was dramatically reduced in HSF1 KD cells and HSF1$^{-/-}$ mouse hepatocytes. We also found that epidermal growth factor-stimulated mitogen-activated protein kinase signaling was impaired in HSF1 KD cells. Clinicopathological analysis demonstrated frequent overexpression of HSF1 in human HCCs. Significant correlations between HSF1 and BAG3 protein levels and prognosis were also observed. In summary, these results identify a mechanistic link between HSF1 and liver tumorigenesis and may provide as a potential molecular target for the development of anti-HCC therapies.

Introduction

Hepatocellular carcinoma (HCC) is one of the most common malignant tumors and the third leading cause of cancer death worldwide (1). Despite marked advances in diagnostic and therapeutic techniques, prognosis remains unsatisfactory for HCC patients (2,3). An understanding of HCC carcinogenesis at the molecular level is thus urgently needed in order to identify novel molecular targets for the development of more effective therapies.

Heat shock factor 1 (HSF1) is the main regulator of the heat shock response, which is involved in protecting cells and organisms from heat, ischemia, inflammation, oxidative stress and other noxious conditions (4,5). Under various forms of physiological stress, HSF1 drives the production of heat shock proteins (HSPs), such as HSP27, HSP70 and HSP90, which act as protein chaperones (5,6). The functions of HSF1 are not limited to increasing the expression of chaperones; HSF1 also modulates the expression of hundreds of genes other than chaperones that are critical for survival under an array of potentially lethal stressors (6–8). As a result, HSF1 influences fundamental cellular processes such as cell cycle control, protein translation, glucose metabolism and proliferation (7–12). In human tumors, constitutive expression of Hsp27, Hsp70 and Hsp90 at high levels predicts poor prognosis and resistance to therapy (13–15). These effects are often attributable to HSF1-dependent mechanisms (16). Thus, as a master regulator of cellular processes, the roles of HSF1 in carcinogenesis and tumor progression are now emerging. Several recent investigations using mouse models have suggested that HSF1 is involved in carcinogenesis (9,17). In clinical samples, HSF1 is often constitutively expressed at high levels in a variety of tumors, including breast cancer (7,18), pancreatic cancer (19), prostate carcinoma (20) and oral squamous cell carcinoma (21).

Hepatocarcinogenesis is a multistep process, in the majority of cases slowly developing within a well-defined etiology of viral infection and chronic alcohol abuse, leading to the chronic hepatitis and cirrhosis that are regarded as preneoplastic stages (22). A great number of factors, receptors and downstream elements of signaling cascades regulate proliferation and apoptosis. Dysregulation of the balance between cell proliferation and apoptosis thus plays a critical role in hepatocarcinogenesis (23,24). Two of the major pathways of cell proliferation and apoptosis are nuclear factor kappa B (NF-κB) signaling and mitogen-activated protein kinase (MAPK) signaling. NF-κB transcription factors are critical regulators of genes involved in inflammation and the suppression of apoptosis. NF-κB has been shown to be instrumental for tumor promotion in colitis-associated cancer and inflammation-associated liver cancer (25,26). Activation of the extracellular signal-regulated kinase (ERK)/MAPK pathway regulates many important cellular processes, such as proliferation, differentiation, angiogenesis, survival and cell adhesion (27). Importantly, the ERK/MAPK pathway is constitutively activated in HCC (28).

The present study investigated the biological influences of HSF1 in HCC cell proliferation and apoptosis involving the NF-κB and MAPK signal pathways. We found that HSF1 deficiency significantly diminished NF-κB and MAPK activation in primary hepatocytes and HCC cells, so HSF1 deficiency inhibited the development of HCC. Furthermore, clinicopathological analysis demonstrated a significant correlation between HSF1 protein level and prognosis. Our results suggest HSF1 as a promising molecular target for the development of anti-HCC therapeutics.

Abbreviations: BAG3, bcl-2-associated athanogene domain 3; EGFR, epidermal growth factor receptor; ERK, extracellular signal-regulated kinase; FACS, fluorescence-activated cell sorting; HCC, hepatocellular carcinoma; HSF1, heat shock factor 1; HSF1 KD, HSF1 knockdown; HSP, heat shock protein; IKKγ, IκB kinase gamma; LPS, lipopolysaccharide; MAPK, mitogen-activated protein kinase; MEK, mitogen-activated protein kinase kinase; mRNA, messenger RNA; NF-κB, nuclear factor kappa B; PCNA, proliferating cell nuclear antigen; SCID, severe combined immune-deficient mice; shRNA, small hairpin RNA; TNF-α, tumor necrosis factor alpha; TUNEL, terminal deoxynucleotidyl transferase-mediated deoxyuridine triphosphate nick-end labeling; WT, wild type.

Materials and methods

Cell cultures and reagents

Human HCC cell lines HepG2, PLC/PRF/5, HLE and HLF were obtained from the American Type Culture Collection. Huh7 was obtained from the Japanese Collection of Research Bioresources Cell Bank (Ibaraki, Japan). KIM-1 and KYN2 were kindly provided by Dr Hirohisa Yano (Department of Pathology, Kurume University, Kurume, Japan). Li7 was kindly provided by Dr Yae Kanai (Division of Molecular Pathology, National Cancer Center Research Institute,

© The Author 2013. Published by Oxford University Press. All rights reserved. For permissions, please email: journals.permissions@oup.com

Downloaded from http://carcin.oxfordjournals.org/ at (D) Hokkaido U Med on February 4, 2015

Tokyo, Japan). HepG2, PLC/PRF/5, Huh7, HLE and HLF cells were maintained in Dulbecco's modified Eagle's medium containing 10% fetal bovine serum. KIM-1 and KYN2 was maintained in RPMI medium containing 10% fetal bovine serum.

Antibodies and chemicals

The antibodies used included: anti-HSF1, ERK1/2, phosphor-ERK1/2, MAPK kinase (MEK), phospho-MEK, phosphor- efficiently activated epidermal growth factor receptor (EGFR), cyclin D1, cdc2, CDK4, phospho-IκBα, IκB kinase gamma (IKKγ), IKKβ, caspase-3 and Bcl-X_L (Cell Signaling Biotechnology, Danvers, MA); anti-HSP90, HSP72, β-actin and proliferating cell nuclear antigen (PCNA) (Santa Cruz Biotechnology, Santa Cruz, CA); anti-EGFR (Millipore, Billerica, MA); anti-HSP70/HSP72 (Enzo Life science, NY); and anti-BAG3 (Abcam, Cambridge, UK).

Biochemical and immunohistochemical analyses

Protein lysates were prepared from tissues and cultured cells, separated by sodium dodecyl sulfate–polyacrylamide gel electrophoresis, transferred onto Immobilon membranes (Millipore) and analyzed by immunoblotting. Total cellular RNA was extracted using Trizol reagent (Invitrogen, Carlsbad, CA), then cDNA was synthesized using SuperScript II (Invitrogen), and expression of specific messenger RNAs (mRNAs) was quantified using real-time PCR and normalized against glyceraldehyde-3-phosphate dehydrogenase mRNA expression. Details of real-time PCR conditions and primer sequences are available in Supplementary Materials and methods, available at *Carcinogenesis* Online. Immunohistochemical staining was performed on formalin-fixed, paraffin-embedded tissue sections using immunoperoxidase methods, as described previously (15). For array analysis, we used the Human WG-6 BeadChip-kit (Illumina, San Diego, CA) in accordance with the instructions from the manufacturer (details are given in Supplementary Materials and methods, available at *Carcinogenesis* Online).

Establishment of HSF1-knockdown cells

A HSF1 small hairpin RNA (shRNA) plasmid and negative control plasmid were purchased from SABiosciences (QIAGEN, Valencia, CA). The shRNA sequences targeting HSF1 were from position 5′-CAGGTTGTTCATAGTCAGAAT-3′ as in the nucleotide sequence of HSF1. As a negative control, a shRNA was designed with the sequence 5′-GGAATCTCATTCGATGCATAC-3′. Transfection was achieved using Oligofectamine reagent (Invitrogen) according to the instructions from the manufacturer. To establish stable knockdown cell lines, shRNA plasmids were transfected into KYN2 cells and cultured in the presence of puromycin (Sigma–Aldrich, St Louis, MO).

Cell proliferation and bromodeoxyuridine assay

Cell proliferation in response to HSF1 silencing was determined by trypan blue exclusion assay. DNA synthesis was determined by bromodeoxyuridine assay according to the instructions from the manufacturer (Roche Diagnostics, Basel, Switzerland). The result was expressed as a percentage of the maximum absorbance at 450 nm, based on three independent experiments. Cells were counted using a Coulter Counter (Beckman Coulter, Pasadena, CA).

Apoptosis assay

Assessment of apoptosis was performed by measuring the intensity of the sub-G_1 peak. For the sub-G_1 peak, HSF1 control KYN2 cells or HSF1-knockdown (HSF1 KD) KYN2 cells were tumor necrosis factor alpha (TNF-α) treatment for 24 h. Cells were treated with propidium iodide and then the sub-G_1 peak was analyzed with a fluorescence-activated cell sorting (FACS) flow cytometer (FACSCalibur; Becton Dickinson, San Jose, CA). Terminal deoxynucleotidyl transferase-mediated deoxyuridine triphosphate nick-end labeling (TUNEL) assay was performed in accordance with the manufacturer's instructions (ApopTag kit; Intergen, Burlington, MA).

Animals

HSF1-deficient ($HSF^{-/-}$) mice have been described previously (29). C57BL/6 wild-type (WT) mice were purchased from CLEA Japan (Tokyo, Japan) for use in the experiments, with primary hepatocytes isolated using a collagenase perfusion method as described in a previous report (26). For orthotopic implantation, C.B-17/Icr-scid/scidJcl [severe combined immune-deficient mice (SCID)] mice were obtained from CLEA Japan. All mice were maintained in filter-topped cages on autoclaved food and water at the University of Hokkaido and the Institute for Adult Diseases, Asahi Life Foundation, according to National Institutes of Health (NIH) guidelines. All experimental protocols were approved by the ethics committee for animal experimentation at Hokkaido University and Asahi Life Foundation. Orthotopic implantation of KYN2 cells and KYN2 transfectants were performed as described previously (30). Briefly, mice were inoculated orthotopically with 5×10^6 HSF1 control ($n = 12$) and HSF1 KD ($n = 12$) cells in 100 μl of phosphate-buffered saline, injected into the liver. Mice were killed 6 weeks after inoculation and autopsies were performed immediately. In the lipopolysaccharide (LPS)/D-galactosamine (GalN)-induced liver injury model, mice were injected intraperitoneally with LPS (20 lg/kg; Sigma) and GalN (1000 mg/kg; Wako, Osaka, Japan) (24).

Patients and tissue samples

For immunohistochemical analysis, a total of 226 adult patients with HCC who underwent curative resection between 1997 and 2006 at Hokkaido University Hospital were enrolled in this study. A preoperative clinical diagnosis of HCC was required to meet the diagnostic criteria of the American Association for the Study of Liver Diseases. Briefly, inclusion criteria were as follows: (i) distinctive pathological diagnosis, (ii) no preoperative anticancer treatment or distant metastases, (iii) curative liver resection (exclusion of extrahepatic tumor spread/metastasis) and (iv) complete clinicopathological and follow-up data. The study protocols were approved by the institutional review board and performed in compliance with the Helsinki of Declaration. Written informed consent was obtained from as many of the patients who were alive as possible (deceased cases were approved for use without written informed consent). Histological diagnosis was made according to World Health Organization criteria. The main clinicopathological features are presented in Table I. During follow-up, clinical evaluations and biochemical tests were performed every 1–3 months. Patients underwent triphasic computed tomography of the liver every 2–3 months.

Statistical analysis

Data are expressed as mean ± standard error of the mean (SEM). Significant differences were detected using non-parametric testing. Correlations between protein expression and clinicopathological features of the specimens were assessed, and the resulting data were analyzed using the χ^2 test and Fisher's exact test. Cumulative survival rate was calculated from the first date of treatment using the Kaplan–Meier life-table method. Differences were evaluated by log-rank testing. Independent factors for survival were assessed with the Cox proportional hazard regression model. Differences between the two groups were analyzed using the log-rank test. Statistical analyses were performed using Stat View software (version 5.0; SAS Institute, Cary, NC). Values of $P < 0.05$ were considered significant.

Results

Effect of HSF1 on tumor growth

We first investigated expression of HSF1 in cultured HCC cell lines. HSF1 expression was detected in all eight HCC cell lines analyzed. KYN2 cells showed significantly higher expression of HSF1 than other cell lines (Figure 1A). To further elucidate the functional role of HSF1 in HCC, we established HSF1 KD KYN2 cells by expressing the shRNA against HSF1 or control shRNA. To evaluate the effects of HSF1 on cell growth, we measured cell numbers at several time points and found that the growth of HSF1 KD cells was significantly inhibited compared with control cells (HSF1 control) (Figure 1B). Cell cycle regulators including PCNA, cyclin D1, cdc2 and CDK4 were suppressed in HSF1 KD cells compared with HSF1 control cells (Figure 1C). These results indicate that HSF1 enhances HCC cell growth. Concordantly, HSF1 KD reduced DNA synthesis as measured by bromodeoxyuridine incorporation (Figure 1D).

To evaluate the effects of HSF1 on HCC *in vivo*, orthotopic xenografts were established by HSF1 control and HSF1 KD KYN2 cells in nude mice. Maximum primary tumor diameters and tumor volumes were significantly decreased in HSF1 KD xenografts compared with HSF1 control ones (Figure 1E), suggesting that HSF1 accelerated HCC tumor growth *in vivo*. We confirmed that the tumor of HSF1 KD cells showed significantly lower expression of HSF1 and PCNA than the tumor of HSF1 control cells (Figure 1E).

We performed gain-of-function experiments for HSF1 *in vitro*. No apparent changes in cell growth were seen with overexpression of HSF1 in HCC cell lines with low HSF1 expression (Supplementary Figure 1, available at *Carcinogenesis* Online), whereas cell growth was reduced in HSF1 KD experiments, as above. Based on these

Downloaded from http://carcin.oxfordjournals.org/ at (D) Hokkaido U Med on February 4, 2015

Table I. HSF1, BAG3 expression and clinicopathological variables in HCC

Parameter	Total	HSF1		*P*	BAG3		*P*
		High	Low		High	Low	
		n = 115	*n* = 111		*n* = 112	*n* = 114	
		≥30	<30		≥25	<25	
Age (years)							
≥60	126	66	60	0.69	59	67	0.42
<60	100	49	51		53	47	
Sex							
Male	185	95	90	0.86	94	91	0.49
Female	41	20	21		18	23	
Etiology							
HBsAg(+)/HCV(−)	85	45	40	0.70	39	46	0.67
HBsAg(−)/HCV(+)	84	43	41		44	40	
HBsAg(+)/HCV(+)	6	4	2		2	4	
HBsAg(−)/HCV(−)	51	23	28		27	24	
Cirrhosis							
Presence	121	64	57	0.59	62	59	0.59
Absence	105	51	54		50	55	
Tumor size (cm)							
<5	149	67	82	0.017*	66	83	0.035*
≥5	77	48	29		46	31	
No. of tumor nodules							
Solitary	168	78	90	0.032*	79	89	0.22
Multiple (≥2)	58	37	21		33	25	
TNM stage							
I and II	139	62	77	0.017*	63	76	0.11
III and IV	87	53	34		49	38	
BCLC stage							
A	81	27	54	<0.001*	32	49	0.065
B	108	64	44		58	50	
C	37	24	13		22	15	
Differentiation							
Well	36	11	25	0.010*	10	26	0.014*
Moderate	143	74	69		75	68	
Poor	47	30	17		27	20	
Capsular formation							
Presence	184	95	89	0.73	91	93	1.0
Absence	42	20	22		21	21	
Vascular invasion							
Present	37	24	13	0.073	22	15	0.21
Absent	189	91	98		90	99	
Serum AFP level							
<20	117	53	64	0.086	52	65	0.14
≥20	109	62	47		60	49	

AFP, alpha-fetoprotein; BCLC, Barcelona Clinic Liver Cancer; HCV, hepatitis C virus; TNM, tumor node metastasis.
*Significant *P* value.

findings, we concluded that HSF1 expression is a necessary condition for cell growth, but it is not a sufficient condition. We, therefore, did not further investigate gain of function of HSF1.

Impaired EGF-mediated MEK/ERK activation in HSF1 KD cells and HSF1$^{-/-}$ hepatocytes

Activation of the MEK/ERK pathway regulates many important cellular processes in carcinogenesis. To further elucidate the function of HSF1 on tumor growth, we investigated the cascade of MAPK. In WT hepatocytes and HSF1 control cells, EGF, a potent activator of MAPK, efficiently activated EGFR, MEK1/2 and ERK1/2 (Figure 2A). In contrast, activation of EGFR, MEK1/2 or ERK1/2 was significantly decreased in HSF-knockout mice (HSF$^{-/-}$) hepatocytes and HSF1 KD cells (Figure 2A and B). Regarding protein levels of EGFR, MEK1/2 and ERK1/2, EGFR protein levels were significantly decreased in HSF1$^{-/-}$ hepatocytes and HSF1 KD compared with controls, whereas other proteins were unchanged (Figure 2A and B). This result was consistent with the previous report (31). Immunohistochemical staining revealed that HSF1 control tumor showed strong phosphorylated ERK1/2 levels, whereas almost no ERK1/2 activation was observed in HSF1 KD tumors (Figure 2C).

Role of HSF1 in TNF-α-induced apoptosis

Since tumor growth inhibition is caused mainly by increased cell death and decreased cellular proliferation, we compared numbers of apoptotic cell deaths in HSF1 control and HSF KD xenografts using the TUNEL assay. Significantly more apoptotic tumor cells were found in HSF1 KD tumors than in HSF1 control tumors (Figure 3A). Next, we examined whether HSF1 was involved in apoptosis *in vitro*. FACS analysis showed very few apoptotic cells in HSF KD or HSF control in the absence of any stimuli. In contrast, treatment with TNF-α, a potent inducer of apoptosis, caused more extensive apoptotic cell death in HSF1 KD cells (23.9%) than in HSF control cells (8.7%) (Figure 3B). Furthermore, we also confirmed increased TNF-α-induced apoptosis in HSF KD cells as determined by TUNEL assay and caspase-3 activation (Figure 3C and D). To examine whether HSF1 is required for TNF-α-induced liver apoptosis *in vivo*, we used an LPS/GalN liver injury model that depends on TNF-α-mediated apoptosis (32). At 7 h LPS/GalN

Downloaded from http://carcin.oxfordjournals.org/ at (D) Hokkaido U Med on February 4, 2015

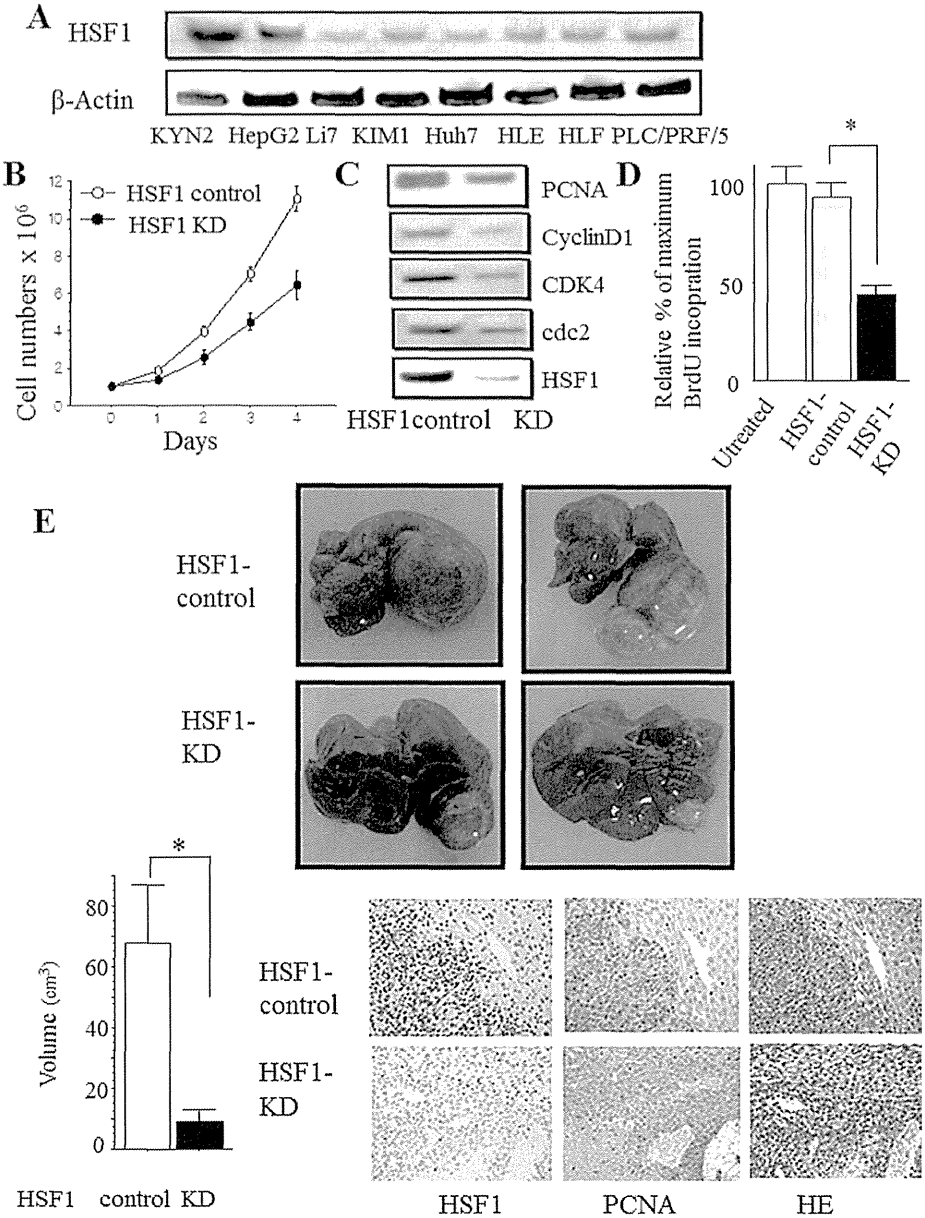

Fig. 1. Role of HSF1 in HCC growth. (**A**) Expression of HSF1 in the eight indicated HCC cell lines was determined by western blot analysis, using β-actin as a control. (**B**) Cell growth of HSF1 control KYN2 cells and HSF1 KD KYN2 cells was measured by counting the number of cells. One representative experiment from three experiments is shown. Data are plotted as mean ± SEM. (**C**) Expression of cell-cycle-related protein in HSF1 control KYN2 cells and HSF1 KD KYN2 cells, as determined by western blot analysis. (**D**) Cells were pulsed with BrdU (10 mmol/l) for 4 h. Optical density values are expressed as a percentage relative to the group expressing control. $^*P < 0.05$. Bars: SEM. (**E**) Growth appearance of HSF1 KD and HSF1 control cells in SCID mice after orthotopic implantation (upper panel). Orthotopic tumor volume was measured. Data are expressed as mean ± SEM (HSF1 control, $n = 12$; HSF1 KD, $n = 12$). $^*P < 0.05$. Bars: SEM (lower left panel). HE and immunohistochemical staining for HSF1 and PCNA (original magnification: ×40): lower right panel. BrdU, bromodeoxyuridine; HE, hematoxylin and eosin.

administration, $HSF^{-/-}$ exhibited marked alanine aminotransferase elevation (Figure 3E), severe histological liver damage and hepatocyte apoptosis compared with WT mice (Figure 3E). This was also in accordance with the notable depression of HSF1 inducing apoptosis *in vitro*.

HSF1 is involved in TNF-α-mediated NF-κB activation

Regarding the association between HSF1 and antiapoptosis, expression of bcl-2-associated athanogene domain 3 (BAG3) was reportedly reduced in HSF1 KD cells compared with control cells (7,11). In addition, microarray array analysis showed that BAG3 was dramatically downregulated in HSF1 KD cells compared with HSF1 control cells (Supplementary Table I, available at *Carcinogenesis* Online). Immunoblot analysis showed that BAG3 protein expression was reduced in $HSF1^{-/-}$ hepatocytes and HSF1 KD cells relative to the respective controls (Figure 4A and B). Meanwhile, activation of IKK and NF-κB pathway represents one of the most important antiapoptotic signals. In addition, BAG3 is also reported to control proteasomal degradation of IKKγ, the regulatory subunit (also called NF-κB essential modulator) of the IKK complex, and

Downloaded from http://carcin.oxfordjournals.org/ at (D) Hokkaido U Med on February 4, 2015

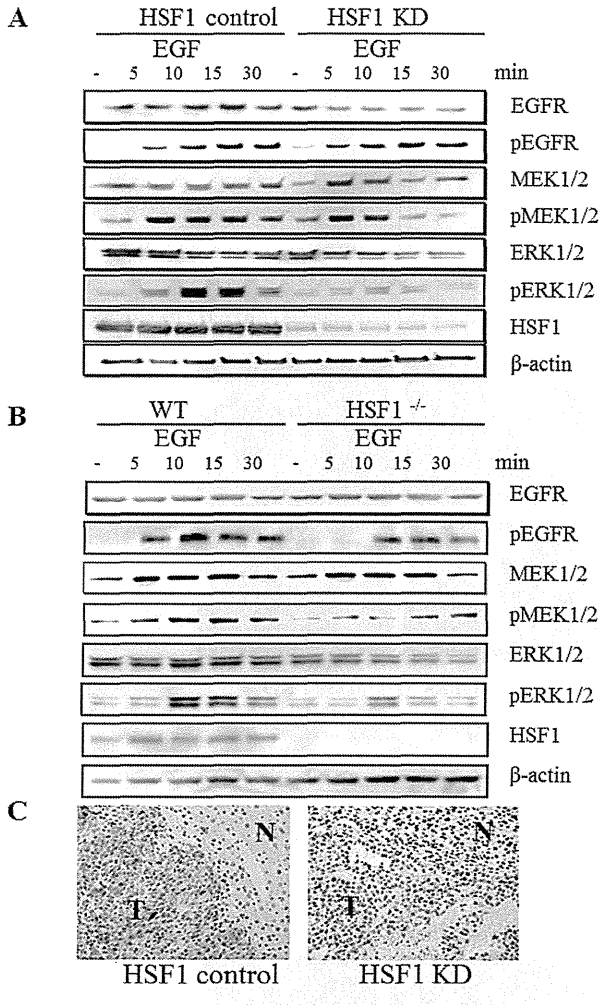

Fig. 2. EGF-mediated MEK/ERK activation is impaired in HSF1 KD cells and HSF1$^{-/-}$ hepatocytes. (**A**) HSF1 control and KD cells were treated with EGF (10 ng/ml), lysed at the indicated times, gel separated and immunoblotted with antibodies against indicated proteins. (**B**) HSF1 WT and HSF$^{-/-}$ hepatocytes were treated with TNF-α (30 ng/ml), lysed in indicated times, gel separated and immunoblotted with antibodies against indicated proteins. (**C**) Representative phosphorylated ERK (p-ERK) staining of orthotopic tumors of HSF1 control and KD cells (original magnification: ×40). N, non-cancerous liver; T, tumor.

NF-κB activity (33). Regarding the NF-κB pathway, NF-κB activation by TNF-α was decreased in HSF1 KD cells compared with the control cells (Figure 4A). In contrast, without any treatment, basal NF-κB activity was very weak and no differences were apparent between HSF1 control cells and HSF1 KD cells (Figure 4A). Consistent with this, microarray analysis showed no apparent differences in the expression of typical NF-κB-regulated genes. We also performed NF-κB pathway analysis and found that the pathway was not overrepresented by the microarray results (Supplementary Figure 2, available at *Carcinogenesis* Online). Next, we investigated whether HSF1 is involved in TNF-α-mediated NF-κB activation and found that phosphorylated Iκk-B (p-IκB), a marker of NF-κB activation, was significantly decreased in HSF$^{-/-}$ hepatocytes and HSF1 KD cells compared with their controls. As expected, IKKγ protein levels were dramatically reduced in HSF1$^{-/-}$ hepatocytes and HSF1 KD cells compared with their controls (Figure 4A and B). To investigate whether decreased IKKγ protein was degraded via proteasome, we used the proteasomal inhibitor, MG-132, and found that protein levels of IKKγ in HSF1 KD cells recovered with the inhibitor, whereas protein expression of BAG3 was unchanged (Figure 4C). Although mRNA levels of BAG3 were significantly downregulated in HSF1 KD cells compared with HSF1 control cells, mRNA levels of IKKγ were not changed (Figure 4D). HSP70 mRNA and protein levels were similar between HSF1 control and HSF1 KD cells (Figure 4A–D). These results suggest that HSF1 positively regulated BAG3 expression, which stabilized the IKKγ protein necessary for NF-κB activation. Immunohistochemical staining revealed that downregulation of HSF1 dramatically reduced BAG3 levels in HSF1 KD xenografts compared with the HSF1 control xenografts.

We performed real-time PCR analysis of the putative NF-κB-regulated antiapoptotic genes. The levels of A20, cellular inhibitor of apoptosis 2 (c-IAP2) RNA expression were decreased in HSF1 KD cells by TNF-α-mediated compared with HSF1 control cells, whereas cylindromatosis, cIAP1 were unchanged (Figure 4E). These results suggest that HSF1 plays an important role in tumor growth via MAPK-mediated cellular proliferation and NF-κB-mediated antiapoptosis.

HSF1 and BAG3 were frequently overexpressed in human HCCs

To analyze the involvement of HSF1 in HCCs, we examined expression levels of HSF1 in human primary HCCs. Immunoblot analysis showed that levels of HSF1 in HCC tissues were significantly higher than in non-cancerous liver tissues in 5 of 10 samples (50%) (Figure 5A). We tested 226 samples from tumor tissues of patients with HCCs by immunohistochemistry. The median percentage of positive cells was 30% (range: 0–90.0%) and we divided patients into two groups of high expressers and low expressers based on the percentage of HSF1-positive cells using a cutoff level of 30%, representing the median value of HSF1. We found that 50.9% (115/226) of tumor samples showed high HSF1 expression. Typical examples of high HSF1 expression samples are shown in Figure 5B. The characteristics of patients in this analysis are shown in Table I. Significant differences were apparent between high and low HSF1 expression groups in terms of tumor size ($P = 0.017$), tumor node metastasis stage ($P = 0.017$), Barcelona Clinic Liver Cancer stage ($P < 0.001$), number of tumor nodules ($P = 0.032$) and histological grade ($P = 0.010$) (Table I), but no significant correlations were observed between HSF1 expression and other clinicopathological variables such as etiology or cirrhosis (Table I). Furthermore, patients with tumors showing HSF1 overexpression displayed significantly shorter overall survival (median: 75.2 months) compared with patients whose tumors showed HSF1 low expression (median: 136.0 months; $P = 0.004$, log-rank test) (Figure 5C). These findings suggest that overexpression of HSF1 was frequently observed in human HCCs, particularly in tumors exhibiting aggressive features.

To explore the pathological relationship between HSF1 and BAG3 in HCC samples, we performed immunohistochemical analysis for BAG3 in 226 HCC samples, which were also analyzed for HSF1 immunohistochemistry. The median percentage of positive cells was 25% (range: 0–85.0%) and we divided them into two groups—high expressers and low expressers—based on the percentage of BAG3-positive cells using a cutoff level of 25%, representing the median value of BAG3. Representative examples of immunohistochemical reactivity for BAG3 are shown in Figure 5B. Expressions of BAG3 protein were significantly increased in HCC specimens, whereas no or only low BAG3 expression was seen in adjacent non-cancerous tissue. BAG3 expression correlated significantly with histological grade ($P = 0.014$), and tumor size ($P = 0.035$), but no significant correlations were observed between BAG3 expression and other clinicopathological variables (Table I). Furthermore, a positive correlation between expressions of HSF1 and BAG3 was found in HCC ($P < 0.05$; Figure 5D) and patients with tumors showing BAG3 overexpression displayed significantly shorter overall survival (median: 84.0 months) compared with those patients whose tumors showed BAG3 low expression (median: 134.2 months; $P = 0.015$, log-rank test) (Figure 5E). Multivariate Cox regression

Downloaded from http://carcin.oxfordjournals.org/ at (D) Hokkaido U Med on February 4, 2015

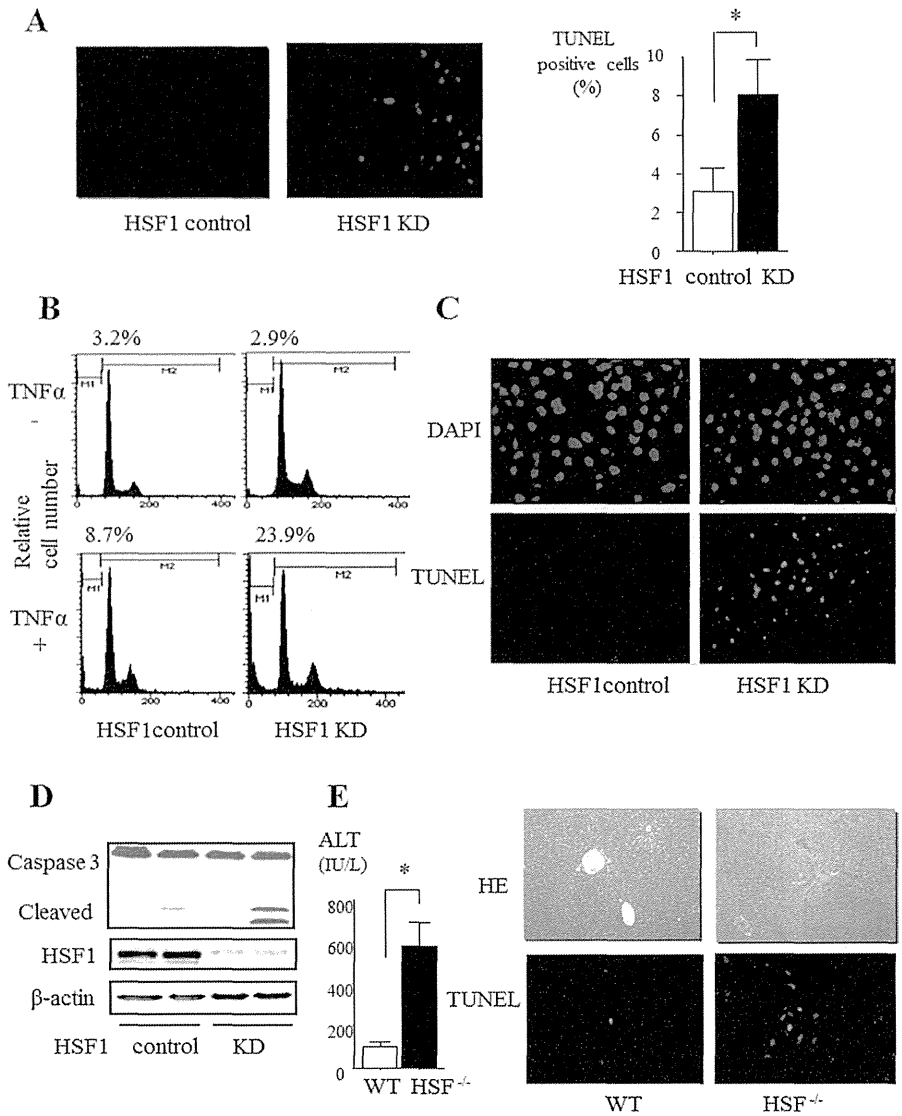

Fig. 3. Antiapoptotic effect of HSF1 in HCC cells and hepatocytes. (**A**) TUNEL staining was performed in tumors of HSF1 control and HSF1 KD cells from orthotopic implanted mice (left panel). TUNEL-positive cells were counted in tumors of HSF1 control and HSF1 KD cells. *$P < 0.05$. Bars: SEM (right panel). (**B**) Apoptotic cells were evaluated by FACS at 24 h after incubation with TNF-α (30 ng/ml). Values indicate percentages of cells with sub-G_1 DNA content. Representative data are shown from three independent experiments. (**C**) TUNEL staining was performed in HSF1 control and KD cells after incubation with TNF-α. (**D**) Protein expressions of caspase 3, HSF1 and β-actin in TNF-α-treated HSF1 control and KD cells were determined by western blot analysis. (**E**) Serum ALT levels 7 h after injection of WT and HSF1$^{-/-}$ mice with LPS (5 μg/kg) and GalN (500 mg/kg). *$P < 0.05$, compared with WT mice (left panel). HE and TUNEL stainings were performed in sections of livers obtained 7 h after injecting LPS (5 μg/kg) and GalN (500 mg/kg) into WT and HSF1$^{-/-}$ mice (right panel). ALT, alanine aminotransferase; DAPI, 4′,6-diamidino-2-phenylindole; HE, hematoxylin and eosin.

analysis identified high HSF1 expression (hazard ratio: 2.07; $P = 0.04$) as an independent prognostic factor for overall survival (Table II).

Discussion

As a master regulator of the heat shock response, HSF1 enhances organism survival and longevity in the face of environmental challenges. However, HSF1 can also act to the detriment of organisms by supporting malignant transformation (34). As reported previously, loss of HSF1 negatively impacts tumorigenesis driven by p53 or Ras mutations (8,16). Since HSF1 does not act as a classic oncogene, the increased resistance to proteotoxic stress induced by HSF1 was suggested to support tumor initiation and growth by enabling cells to accommodate the genetic alterations that accumulate during malignancy (35). However, the specific mechanisms by which HSF1 may support the growth of tumors are not well understood. Here, we have demonstrated that HSF1 has detrimental effects on liver tumor growth. We also proposed that the antiapoptotic effect of HSF1 may play a role in HCC tumor growth.

To clarify the mechanisms underlying this effect, we investigated associations between HSF1 and the NF-κB signaling pathway. Although, in a previous study, heat shock blocked the degradation of IκB (36) and nuclear translocation of NF-κB, the recent literature has reported that the presence of constitutively active HSF1 does not block TNF-α-induced activation of the NF-κB pathway or expression of a set of NF-κB-dependent genes (37). The current study established HSF1 KD cells and showed that HSF1 was necessary for TNF-α-induced NF-κB activation. We analyzed the function of BAG3 as a candidate for the molecule connecting HSF1 with NF-κB activation. BAG3 has reportedly been characterized by the

Downloaded from http://carcin.oxfordjournals.org/ at (D) Hokkaido U Med on February 4, 2015

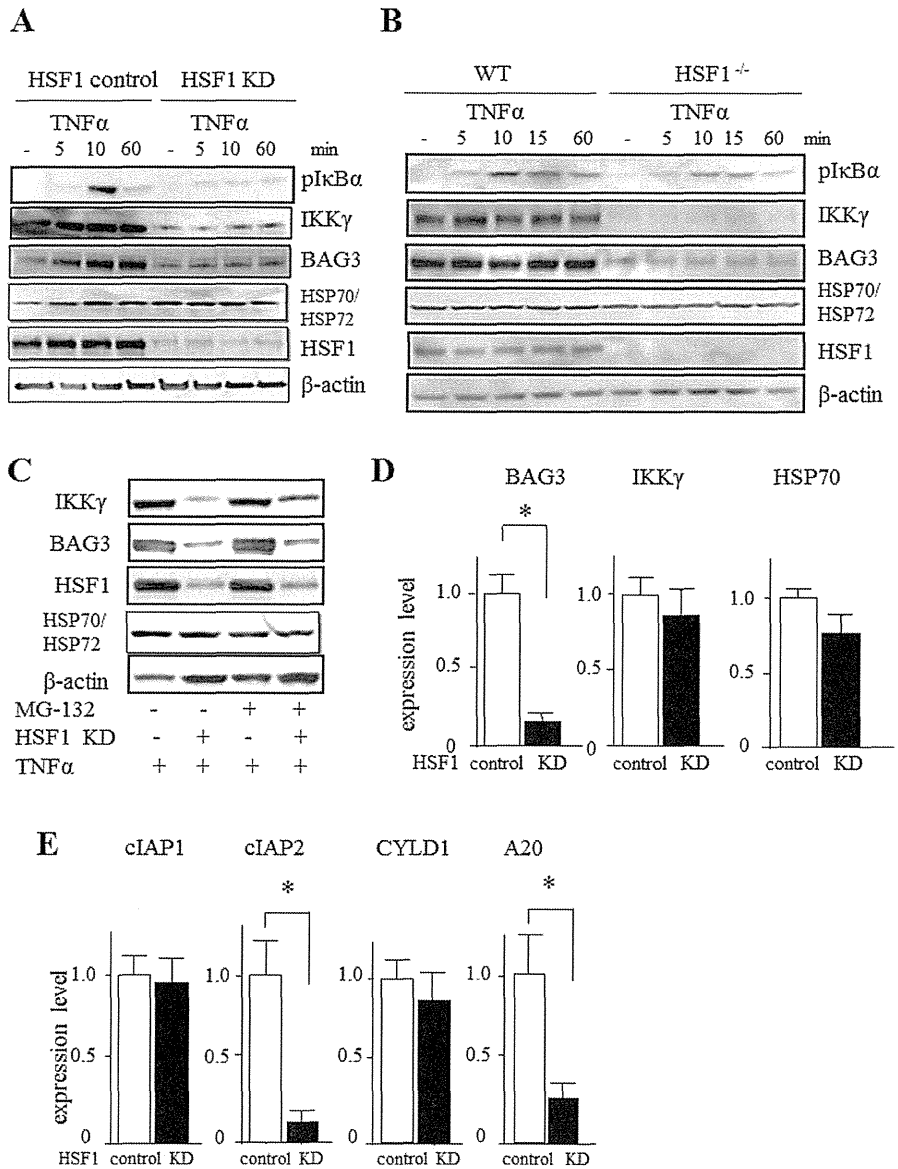

Fig. 4. HSF1 is involved in TNF-α-mediated NF-κB activation. (**A**) HSF1 control and KD cells were treated with TNF-α (30 ng/ml), lysed at the indicated times, gel separated and immunoblotted with antibodies against the indicated proteins. (**B**) HSF1 WT and HSF$^{-/-}$ hepatocytes treated with TNF-α (30 ng/ml), lysed at the indicated times, gel separated and immunoblotted with antibodies against the indicated proteins. (**C**) HSF1 control and KD cells were treated with TNF-α (30 ng/ml) with or without MG-132, lysed at 24 h, gel separated and immunoblotted with antibodies against indicated proteins. (**D**) Relative mRNA levels for BAG3, IKKγ and HSP70 in HSF1 control and KD cells determined by real-time PCR. Data are expressed as mean ± SEM ($n = 4$ per group). *$P < 0.05$. Bars: SEM. (**E**) Relative mRNA levels for antiapoptosis-related gene in HSF1 control and KD cells as determined by real-time PCR. Data are expressed as mean ± SEM ($n = 4$ per group). *$P < 0.05$. Bars: SEM. CYLD, cylindromatosis.

interaction with a variety of partners (Raf-1, steroid hormone receptors and HSP70) and is involved in regulating a number of cellular processes, particularly those associated with antiapoptosis (38). This molecule was expressed in response to stressful stimuli in a number of normal cell types and appears constitutively in a variety of tumors (33,39), and gene expression is regulated by HSF1 (40). In addition, knockdown of BAG3 protein decreased IKKγ levels, increasing tumor cell apoptosis and inhibiting tumor growth (33). Based on these considerations, we investigated whether attenuating HSF1 would enhance IKKγ protein expression, and data with MG-132 show that proteasomal degradation of IKKγ is enhanced in HSF1 KD cells. In addition, knowledge of the role BAG3 plays in preventing the proteasomal turnover of certain proteins suggests that the loss of BAG3 in HSF1 KD cells may be responsible for the enhanced turnover of IKKγ in this setting.

NF-κB activation is a master regulatory step in antiapoptosis. Several mechanisms have been reported regarding this antiapoptotic effect of NF-κB activation (41). NF-κB exerts its prosurvival activity primarily through the induction of target genes, the products of which inhibit components of the apoptotic machinery. These include Bcl-X_L and c-IAP (41), which binds directly to and inhibits the effect of caspases. This study showed that inactivation of NF-κB promoted apoptotic effects against TNF-α in HSF1$^{-/-}$ hepatocytes and HSF1 KD HCC cells. Real-time PCR analyses indicated that expression levels of apoptosis-related genes such as A20 and c-IAP2 were decreased by inhibition of NF-κB activation, whereas apoptosis-related genes such

Downloaded from http://carcin.oxfordjournals.org/ at (D) Hokkaido U Med on February 4, 2015

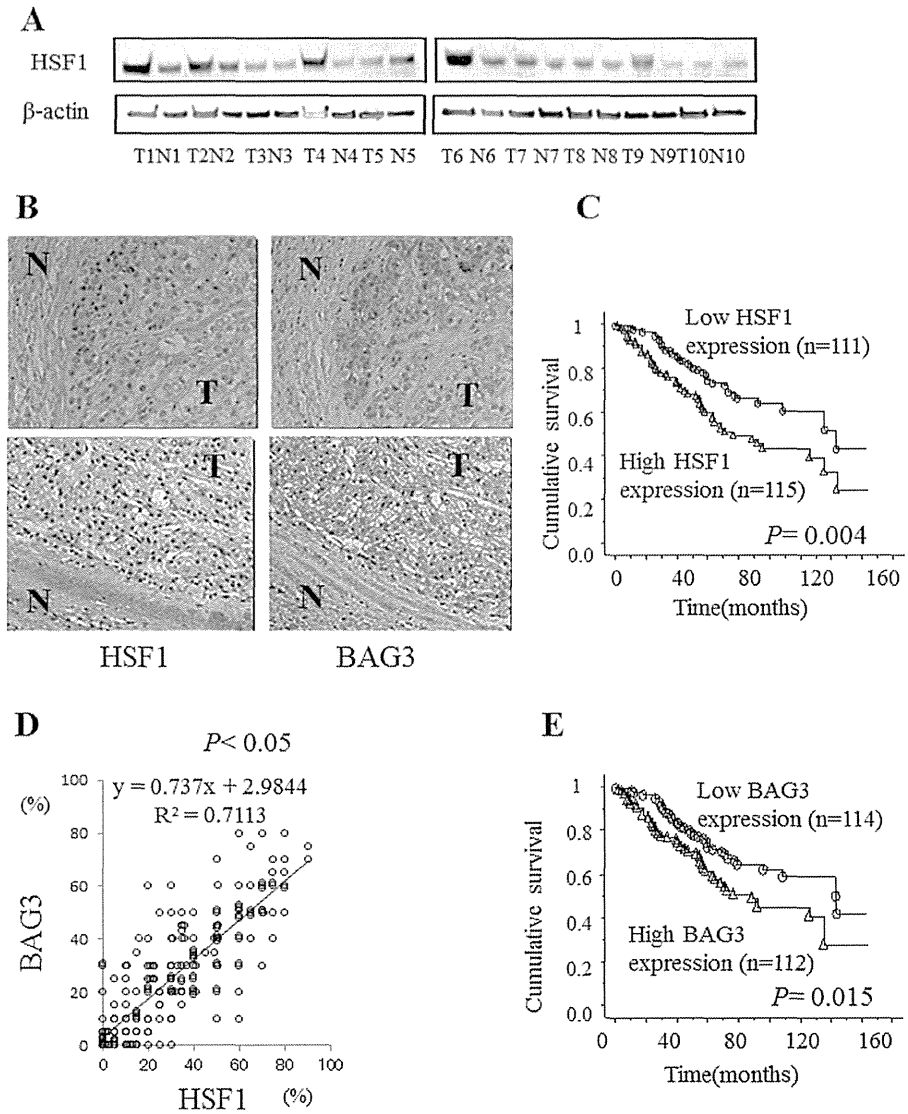

Fig. 5. *Overexpression of HSF1 protein in human HCCs and pathological relationship between HSF1 and BAG3 in HCC samples.* (**A**) *HSF1 protein* expression was determined in paired samples of human non-neoplastic liver and HCC by western blot, using β-actin as a control. N, non-cancerous liver; T, tumor. (**B**) Representative HSF1 and BAG3 staining of HCC and surrounding tissue. (**C**) Correlation of HSF1 overexpression with overall survival rates of patients. (**D**) Relationship between BAG3 and HSF1 expression in HCC. Scatterplot of BAG3 versus HSF1 with regression line displaying a correlation according to Spearman's correlation coefficient ($P < 0.01$). (**E**) Correlation of BAG3 overexpression with overall survival rates of patients.

as cIAP1 and cylindromatosis, which are known to be regulated by NF-κB activation, were apparently unaffected. Whether gene expression regulated by NF-κB activity differs between inducible and basal activation remains to be determined.

Regarding the relationship between HSF1 and HCC development, HSF1-deficient mice recently revealed dramatically reduced numbers and sizes of tumors compared with WT controls when tumors were induced by the chemical carcinogen, diethylnitrosamine. The same study suggested that the presence of extensive pathology associated with severe steatosis by diethylnitrosamine was prevented by HSF1 deletion and may be associated with reduced HCC development (42). On the other hand, ablation of IKKγ in liver parenchymal cells caused spontaneous development of HCC in mice, with tumor development preceded by steatohepatitis (43). Based on these observations, we assume that reductions in diethylnitrosamine-induced HCC development among HSF1-deficient mice may be associated with reduced expression of IKKγ, the reduction of which caused the steatosis.

BAG3 is a critical regulator of apoptosis in HSF1-deficient hepatocytes and HSF1 KD HCC cells. Moreover, the relationship between HSF1 and BAG3 has been shown not only in cell cultures and mouse models, but also in human HCC tissue samples; a correlation between HSF1 expression and BAG3 expression was found in HCC. Clinicopathological features and biological results provide a mechanistic link between HSF1 and HCC development via BAG3.

As for the ERK signal, a previous study demonstrated that impairment of JNK and ERK signaling in HSF1$^{-/-}$ MEF cells was caused in part by the reduced expression of EGFR (33). We showed a slight decrease in expression of EGFR among HSF1-deficient hepatocytes and HSF1 KD cells. On the other hand, the level of reduced activation of ERK, as a downstream molecule of EGFR, was larger than expected. However, the detailed mechanisms by which HSF1 regulates MAPK need further investigation.

In conclusion, we found that HSF1 deficiency significantly diminished NF-κB and MAPK activation in HCC hepatocytes and

Downloaded from http://carcin.oxfordjournals.org/ at (D) Hokkaido U Med on February 4, 2015

Table II. Multivariate analysis with a Cox proportional hazards regression model

Characteristic	Univariate analysis	Multivariate analysis	Hazard ratio (95% CI)
Age (≥60 years)	0.22	0.15	
Gender (male)	0.92	0.53	
HCV status (positive)	0.28	0.82	
Cirrhosis (positive)	0.15	0.066	
Tumor size (≥50 mm)	<0.01*	0.011*	2.21 (1.18–4.12)
No. of tumor nodule (multiple)	<0.01*	<0.01*	2.67 (1.38–5.62)
Tumor differentiation (poor)	<0.01*	0.031*	2.34 (1.33–4.11)
Capsular formation (absence)	0.18	0.36	
Vascular invasion (presence)	0.062	0.10	
TNM stage (III + IV versus I + II)	<0.01*	0.020*	2.35 (1.14–4.82)
AFP (≥20 ng/ml)	0.18	0.36	
HSF1 expression (high)	0.018*	0.040*	2.07 (1.22–3.50)
BAG3 expression (high)	0.043*	0.056	

AFP, alpha-fetoprotein; CI, confidence interval; HCV, hepatitis C virus; TNM, tumor node metastasis.
*Significant *P* value.

HCC cells; accordingly, HSF1 deficiency inhibited the development of HCC. Furthermore, clinicopathological analysis demonstrated a significant correlation between HSF1 or BAG3 protein levels and prognosis. Our results demonstrate the importance of HSF1 in human HCCs and suggest inhibition of HSF1 as a novel strategy to target that subset of HCC patients in whom this protein is overexpressed.

Supplementary material

Supplementary Materials and methods, Table I and Figures 1 and 2 can be found at http://carcin.oxfordjournals.org/

Funding

Ministry of Education, Culture, Sports, Science and Technology, Japan (to N.S.); Japan Society for the Promotion of Science (24390185, 24659359); Ministry of Health, Labour and Welfare Japan; Japan Health Sciences Foundation; grants-in-aid for scientific research (22300317) and Uehara Memorial Foundation (to S.M.).

Conflict of Interest Statement: None declared.

References

1. El-Serag,H.B. (2012) Epidemiology of viral hepatitis and hepatocellular carcinoma. *Gastroenterology*, **142**, 1264–1273.e1.
2. Cheng,A.L. *et al.* (2009) Efficacy and safety of sorafenib in patients in the Asia-Pacific region with advanced hepatocellular carcinoma: a phase III randomised, double-blind, placebo-controlled trial. *Lancet Oncol.*, **10**, 25–34.
3. Breuhahn,K. *et al.* (2011) Strategies for hepatocellular carcinoma therapy and diagnostics: lessons learned from high throughput and profiling approaches. *Hepatology*, **53**, 2112–2121.
4. Pirkkala,L. *et al.* (2001) Roles of the heat shock transcription factors in regulation of the heat shock response and beyond. *FASEB J.*, **15**, 1118–1131.
5. Sorger,P.K. (1991) Heat shock factor and the heat shock response. *Cell*, **65**, 363–366.
6. Guertin,M.J. *et al.* (2010) Chromatin landscape dictates HSF binding to target DNA elements. *PLoS Genet.*, **6**, e1001114.
7. Mendillo,M.L. *et al.* (2012) HSF1 drives a transcriptional program distinct from heat shock to support highly malignant human cancers. *Cell*, **150**, 549–562.
8. Page,T.J. *et al.* (2006) Genome-wide analysis of human HSF1 signaling reveals a transcriptional program linked to cellular adaptation and survival. *Mol. Biosyst.*, **2**, 627–639.
9. Dai,C. *et al.* (2007) Heat shock factor 1 is a powerful multifaceted modifier of carcinogenesis. *Cell*, **130**, 1005–1018.
10. Hayashida,N. *et al.* (2006) A novel HSF1-mediated death pathway that is suppressed by heat shock proteins. *EMBO J.*, **25**, 4773–4783.
11. Jacobs,A.T. *et al.* (2007) Heat shock factor 1 attenuates 4-hydroxynonenal-mediated apoptosis: critical role for heat shock protein 70 induction and stabilization of Bcl-XL. *J. Biol. Chem.*, **282**, 33412–33420.
12. Vydra,N. *et al.* (2006) Spermatocyte-specific expression of constitutively active heat shock factor 1 induces HSP70i-resistant apoptosis in male germ cells. *Cell Death Differ.*, **13**, 212–222.
13. Neckers,L. *et al.* (2012) Hsp90 molecular chaperone inhibitors: are we there yet? *Clin. Cancer Res.*, **18**, 64–76.
14. Khalil,A.A. *et al.* (2011) Heat shock proteins in oncology: diagnostic biomarkers or therapeutic targets? *Biochim. Biophys. Acta*, **1816**, 89–104.
15. Chuma,M. *et al.* (2003) Expression profiling in multistage hepatocarcinogenesis: identification of HSP70 as a molecular marker of early hepatocellular carcinoma. *Hepatology*, **37**, 198–207.
16. Cai,L. *et al.* (2003) The tumor-selective over-expression of the human Hsp70 gene is attributed to the aberrant controls at both initiation and elongation levels of transcription. *Cell Res.*, **13**, 93–109.
17. Min,J.N. *et al.* (2007) Selective suppression of lymphomas by functional loss of Hsf1 in a p53-deficient mouse model for spontaneous tumors. *Oncogene*, **26**, 5086–5097.
18. Santagata,S. *et al.* (2011) High levels of nuclear heat-shock factor 1 (HSF1) are associated with poor prognosis in breast cancer. *Proc. Natl Acad. Sci. USA*, **108**, 18378–18383.
19. Dudeja,V. *et al.* (2011) Prosurvival role of heat shock factor 1 in the pathogenesis of pancreatobiliary tumors. *Am. J. Physiol. Gastrointest. Liver Physiol.*, **300**, G948–G955.
20. Hoang,A.T. *et al.* (2000) A novel association between the human heat shock transcription factor 1 (HSF1) and prostate adenocarcinoma. *Am. J. Pathol.*, **156**, 857–864.
21. Ishiwata,J. *et al.* (2012) State of heat shock factor 1 expression as a putative diagnostic marker for oral squamous cell carcinoma. *Int. J. Oncol.*, **40**, 47–52.
22. Kojiro,M. *et al.* (2009) Pathologic diagnosis of early hepatocellular carcinoma: a report of the international consensus group for hepatocellular neoplasia. *Hepatology*, **49**, 658–664.
23. Fabregat,I. *et al.* (2007) Survival and apoptosis: a dysregulated balance in liver cancer. *Liver Int.*, **27**, 155–162.
24. Nakagawa,H. *et al.* (2011) Apoptosis signal-regulating kinase 1 inhibits hepatocarcinogenesis by controlling the tumor-suppressing function of stress-activated mitogen-activated protein kinase. *Hepatology*, **54**, 185–195.
25. Sun,B. *et al.* (2008) NF-kappaB signaling, liver disease and hepatoprotective agents. *Oncogene*, **27**, 6228–6244.
26. Maeda,S. *et al.* (2005) IKKbeta couples hepatocyte death to cytokine-driven compensatory proliferation that promotes chemical hepatocarcinogenesis. *Cell*, **121**, 977–990.
27. Beeram,M. *et al.* (2005) Raf: a strategic target for therapeutic development against cancer. *J. Clin. Oncol.*, **23**, 6771–6790.
28. Whittaker,S. *et al.* (2010) The role of signaling pathways in the development and treatment of hepatocellular carcinoma. *Oncogene*, **29**, 4989–5005.
29. Inouye,S. *et al.* (2003) Activation of heat shock genes is not necessary for protection by heat shock transcription factor 1 against cell death due to a single exposure to high temperatures. *Mol. Cell. Biol.*, **23**, 5882–5895.
30. Chuma,M. *et al.* (2004) Overexpression of cortactin is involved in motility and metastasis of hepatocellular carcinoma. *J. Hepatol.*, **41**, 629–636.
31. O'Callaghan-Sunol,C. *et al.* (2006) Heat shock transcription factor (HSF1) plays a critical role in cell migration via maintaining MAP kinase signaling. *Cell Cycle*, **5**, 1431–1437.

Downloaded from http://carcin.oxfordjournals.org/ at (D) Hokkaido U Med on February 4, 2015

32. Nowak,M. *et al.* (2000) LPS-induced liver injury in D-galactosamine-sensitized mice requires secreted TNF-alpha and the TNF-p55 receptor. *Am. J. Physiol. Regul. Integr. Comp. Physiol.*, **278**, R1202–R1209.
33. Ammirante,M. *et al.* (2010) IKK{gamma} protein is a target of BAG3 regulatory activity in human tumor growth. *Proc. Natl Acad. Sci. USA*, **107**, 7497–7502.
34. Meng,L. *et al.* (2010) Heat-shock transcription factor HSF1 has a critical role in human epidermal growth factor receptor-2-induced cellular transformation and tumorigenesis. *Oncogene*, **29**, 5204–5213.
35. Solimini,N.L. *et al.* (2007) Non-oncogene addiction and the stress phenotype of cancer cells. *Cell*, **130**, 986–988.
36. Malhotra,V. *et al.* (2002) Heat shock inhibits activation of NF-kappaB in the absence of heat shock factor-1. *Biochem. Biophys. Res. Commun.*, **291**, 453–457.
37. Janus,P. *et al.* (2011) NF-κB signaling pathway is inhibited by heat shock independently of active transcription factor HSF1 and increased levels of inducible heat shock proteins. *Genes Cells*, **16**, 1168–1175.
38. Rosati,A. *et al.* (2011) BAG3: a multifaceted protein that regulates major cell pathways. *Cell Death Dis.*, **2**, e141.
39. Homma,S. *et al.* (2006) BAG3 deficiency results in fulminant myopathy and early lethality. *Am. J. Pathol.*, **169**, 761–773.
40. Franceschelli,S. *et al.* (2008) Bag3 gene expression is regulated by heat shock factor 1. *J. Cell. Physiol.*, **215**, 575–577.
41. Luo,J.L. *et al.* (2005) IKK/NF-kappaB signaling: balancing life and death–a new approach to cancer therapy. *J. Clin. Invest.*, **115**, 2625–2632.
42. Jin,X. *et al.* (2011) Heat shock transcription factor 1 is a key determinant of HCC development by regulating hepatic steatosis and metabolic syndrome. *Cell Metab.*, **14**, 91–103.
43. Luedde,T. *et al.* (2007) Deletion of NEMO/IKKgamma in liver parenchymal cells causes steatohepatitis and hepatocellular carcinoma. *Cancer Cell*, **11**, 119–132.

Received December 4, 2012; revised August 22, 2013; accepted August 28, 2013

Downloaded from http://carcin.oxfordjournals.org/ at (D) Hokkaido U Med on February 4, 2015

jbc The Journal of Biological Chemistry
AFFINITY SITES
ASBMB American Society for Biochemistry and Molecular Biology

Microbiology:

Dysregulation of Retinoic Acid Receptor Diminishes Hepatocyte Permissiveness to Hepatitis B Virus Infection through Modulation of NTCP Expression

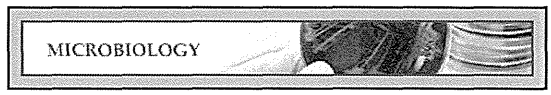

Senko Tsukuda, Koichi Watashi, Masashi Iwamoto, Ryosuke Suzuki, Hideki Aizaki, Maiko Okada, Masaya Sugiyama, Soichi Kojima, Yasuhito Tanaka, Masashi Mizokami, Jisu Li, Shuping Tong and Takaji Wakita

J. Biol. Chem. published online December 30, 2014

Access the most updated version of this article at doi: 10.1074/jbc.M114.602540

Find articles, minireviews, Reflections and Classics on similar topics on the JBC Affinity Sites.

Alerts:
- When this article is cited
- When a correction for this article is posted

Click here to choose from all of JBC's e-mail alerts

This article cites 0 references, 0 of which can be accessed free at
http://www.jbc.org/content/early/2014/12/30/jbc.M114.602540.full.html#ref-list-1

Downloaded from http://www.jbc.org/ at National Institute of Infectious Diseases LIBRARY on February 13, 2015

JBC Papers in Press. Published on December 30, 2014 as Manuscript M114.602540
The latest version is at http://www.jbc.org/cgi/doi/10.1074/jbc.M114.602540

Dysregulation of retinoic acid receptor diminishes hepatocyte permissiveness to hepatitis B virus infection through modulation of NTCP expression

Senko Tsukuda[1,2], Koichi Watashi[1]*, Masashi Iwamoto[1], Ryosuke Suzuki[1], Hideki Aizaki[1], Maiko Okada[3], Masaya Sugiyama[4], Soichi Kojima[2], Yasuhito Tanaka[5], Masashi Mizokami[4], Jisu Li[6], Shuping Tong[6], Takaji Wakita[1]

[1]Department of Virology II, National Institute of Infectious Diseases, Tokyo, 162-8640, Japan, [2]Micro-signaling Regulation Technology Unit, RIKEN Center for Life Science Technologies, Wako, 351-0198, Japan. [3]Department of Translational Oncology, St. Marianna University School of Medicine, Kawasaki, 216-8511, Japan, [4]The Research Center for Hepatitis and Immunology, National Center for Global Health and Medicine, Ichikawa, 272-8516, Japan, [5]Department of Virology and Liver Unit, Nagoya City University Graduate School of Medicinal Sciences, Nagoya, 467-8601, Japan, [6]Liver Research Center Rhode Island Hospital, Warren Alpert School of Medicine, Brown University, Province, Rhode Island, 02912, USA.

Running Title: Retinoids reduced HBV susceptibility by downregulating NTCP

***Address correspondence to:** Koichi Watashi, Ph.D.
Department of Virology II, National Institute of Infectious Diseases
1-23-1 Toyama, Shinjuku-ku, Tokyo, 162-8640, Japan
Tel: +81-3-5285-1111; Fax: +81-3-5285-1161
E-mail: kwatashi@nih.go.jp

Keywords: hepatitis virus, transporter, retinoid, transcription, chemical biology, HBV, infection, RAR, permissive, NTCP

Downloaded from http://www.jbc.org/ at National Institute of Infectious Diseases LIBRARY on February 13, 2015

Copyright 2014 by The American Society for Biochemistry and Molecular Biology, Inc.

Background: Host factors regulating hepatitis B virus (HBV) entry receptors are not well defined.
Results: Chemical screening identified that retinoic acid receptor (RAR) regulates sodium taurocholate cotransporting polypeptide (NTCP) expression and supports HBV infection.
Conclusion: RAR regulates NTCP expression, and thereby supports HBV infection.
Significance: RAR regulation of NTCP can be a target for preventing HBV infection.

Abstract

Sodium taurocholate cotransporting polypeptide (NTCP) is an entry receptor for hepatitis B virus (HBV) and is regarded as one of the determinants that confer HBV permissiveness to host cells. However, how host factors regulate the ability of NTCP to support HBV infection is largely unknown. We aimed to identify the host signaling that regulated NTCP expression and, thereby, permissiveness to HBV. Here, a cell-based chemical screening method identified that Ro41-5253 decreased host susceptibility to HBV infection. Pretreatment with Ro41-5253 inhibited the viral entry process without affecting HBV replication. Intriguingly, Ro41-5253 reduced expression of both NTCP mRNA and protein. We found that retinoic acid receptor (RAR) regulated the promoter activity of the human NTCP (hNTCP) gene, and that Ro41-5253 repressed the hNTCP promoter by antagonizing RAR. RAR recruited to the hNTCP promoter region, and nt -112 to -96 of the hNTCP was suggested to be critical for RAR-mediated transcriptional activation. HBV susceptibility was decreased in pharmacologically RAR-inactivated cells. CD2665 showed a stronger anti-HBV potential and disrupted the spread of HBV infection that was achieved by continuous reproduction of whole HBV life cycle. In addition, this mechanism was significant for drug development, as antagonization of RAR blocked infection of multiple HBV genotypes and also a clinically relevant HBV mutant which was resistant to nucleoside analogs. Thus, RAR is crucial for regulating NTCP expression which determines permissiveness to HBV infection. This is the first demonstration showing host regulation of NTCP to support HBV infection.

Introduction

Hepatitis B virus (HBV) infection is a major public health problem, as the virus chronically infects approximately 240 million people worldwide (1-3). Chronic HBV infection elevates the risk for developing liver cirrhosis and hepatocellular carcinoma (4-6). Currently, two classes of antiviral agents are available to combat chronic HBV infection. First, interferon (IFN)-based drugs including IFNα and pegylated-IFNα modulate host immune function and/or directly inhibit HBV replication in hepatocytes (7,8). However, the antiviral efficacy of IFN-based drugs is restricted to less than 40% (9,10). Second, nucleos(t)ide analogues including lamivudine (LMV), adefovir, entecavir (ETV), tenofovir and telbivudine suppress HBV by inhibiting the viral reverse transcriptase (11,12). Although they can provide significant clinical improvement, long-term therapy with nucleos(t)ide analogues often results in the selection of drug resistant mutations in the target gene, which limits the treatment outcome. For example, in patients treated with ETV, at least three mutations can arise in the reverse transcriptase sequence at of the polymerase L180M, M204V plus either one of T184, S202 or M250 codon changes to acquire drug resistance (13). Therefore, development of new anti-HBV agents targeting other molecules requires elucidation of the molecular mechanisms underlying the HBV life cycle.

HBV infection of hepatocytes involves multiple steps. The initial viral attachment to the host cell surface starts with a low affinity binding involving heparan sulfate proteoglycans, and the following viral entry is mediated by a specific interaction between HBV and its host receptor(s) (14). Recently, sodium taurocholate cotransporting polypeptide (NTCP) was reported as a functional receptor for HBV (15). NTCP interacts with HBV large surface protein (HBs) to mediate viral attachment and the subsequent entry step. NTCP, also known as solute carrier protein 10A1 (SLC10A1), is physiologically a sodium-dependent transporter for bile salts located on the basolateral membrane of hepatocytes (16). In the liver, hepatocytes take up bile salts from the portal blood and secrete them into bile for enterohepatic

Downloaded from http://www.jbc.org/ at National Institute of Infectious Diseases LIBRARY on February 13, 2015

circulation, and NTCP-mediated uptake of bile salts into hepatocytes occurs largely in a sodium-dependent manner. Although NTCP is abundant in freshly isolated primary hepatocytes, it is weakly or no longer expressed in most cell lines such as HepG2 and Huh-7, and these cells rarely support HBV infection (17,18). In contrast, primary human hepatocytes, primary tupaia hepatocyte and differentiated HepaRG cells, which are susceptible to HBV infection, express significant levels of NTCP (19). Thus, elucidation of the regulatory mechanisms for NTCP gene expression is important for understanding the HBV susceptibility of host cells as well as for developing a new anti-HBV strategy. HBV entry inhibitors are expected to be useful for preventing *de novo* infection after liver transplantation, for post-exposure prophylaxis, or vertical transmission by short-term treatment (20,21).

In this study, we used a HepaRG-based HBV infection system to screen for small molecules capable of decreasing HBV infection. We found that pretreatment of host cells with Ro41-5253 reduced HBV infection. Ro41-5253 reduced NTCP expression by repressing the promoter activity of the human NTCP (hNTCP) gene. Retinoic acid receptor (RAR) played a crucial role in regulating the promoter activity of hNTCP, and Ro41-5253 antagonized RAR to reduce NTCP transcription and consequently HBV infection. This and other RAR inhibitors showed anti-HBV activity against different genotypes and an HBV nucleoside analog-resistant mutant, and moreover inhibited the spread of HBV. This study clarified one of the mechanisms for gene regulation of NTCP to support HBV permissiveness, and also suggests a novel concept whereby manipulation of this regulation machinery can be useful for preventing HBV infection.

Experimental Procedures

Regents

Heparin was obtained from Mochida Pharmaceutical. Lamivudine, cyclosporin A, all-trans retinoic acid (ATRA), and TO901317 were obtained from Sigma. Entecavir was obtained from Santa Cruz Biotechnology. Ro41-5253 was obtained from Enzo life sciences. PreS1-lipopeptide and FITC-labeled preS1 were synthesized by CS bio. IL-1b was purchased from Peprotech. CD2665, BMS195614, BMS493, and MM11253 were purchased from Tocris Bioscience.

Cell culture

HepaRG cells (BIOPREDIC) and primary human hepatocytes (Phoenixbio) were cultured as described previously (19). HepG2 and HepAD38 cells (kindly provided by Dr. Christoph Seeger at Fox Chase Cancer Center) (22), were cultured with DMEM/F-12+GlutaMax (Invitrogen) supplemented with 10 mM HEPES (Invitrogen), 200 units/ml penicillin, 200 μg/ml streptomycin, 10% FBS, and 5 μg/ml insulin. HuS-E/2 cells (kindly provided by Dr. Kunitada Shimotohno at National Center for Global Health and Medicine) were cultured as described previously (23).

Plasmid construction

phNTCP-Gluc, pTK-Rluc was purchased from Genecopoeia and Promega, respectively. pRARE-Fluc was generated as described (25). For constructing phNTCP-Gluc carrying a mutation in a putative RARE (nt -491 to -479), the DNA fragments were amplified by PCR using phNTCP-Gluc as a template with primer sets F1; 5'-CAGATCTTGGAATTCCCAAAATC-3' and 5'-GAGGGGATGTGTCCATTGAAATGTTAAT GGGAGCTGAGAGGATGCCAGTATCCTCCC T-3', and with primer sets 5'-CTCTCAGCTCCCATTAACATTTCAATGG ACACATCCCCTCCTGGAGGCCAGTGACATT -3' and R6: 5'-CTCGGTACCAAGCTTTCCTTGTT-3'. The resultant products were further amplified by PCR with F1 and R6, and then inserted into the EcoRI/HindIII sites of phNTCP-Gluc to generate phNTCP Mut(-491~-479)-Gluc. Other promoter mutants were prepared by the same method using the primer sets, F1 and 5'-GTGGGTTATCATTTGTTTCCCGAAAACATT AGAGTGAAAGGAGCTGGGTGTTGCCTTTG G-3', 5'-TCCTTTCACTCTAATGTTTTCGGGAAACAA ATGATAACCCACTGGACATGGGGAGGGCA C-3' and R6 for -368~-356; F1 and 5'-AATCTAGGTCCAGCCTATTTAAGTCCCTAA ATTTCCTTTTCCCAGCTCCGCTCTTGATTCC TT-3', 5'-CTGGGAAAAGGAAATTTAGGGACTTAAAT

Downloaded from http://www.jbc.org/ at National Institute of Infectious Diseases LIBRARY on February 13, 2015

AGGCTGGACCTAGATTCAGGTGGGCCCTG GGCAG-3' and R6 for -274 ~ -258; F1 and 5'-TTCTGGGCTTATTTCTATATTTTGCAATCCA CTGAGTGTGCCTCATGGGCATTCATTC-3', 5'-CACACTCAGTGGATTGCAAAATATAGAAA TAAGCCCAGAAGCAGCAAAGTGACAAGGG -3' and R6 for -179 ~ -167; F1 and 5'-AGCTCTCCCAAGCTCAAAGATAAATGCTA GTTTCCTGGGTGCTACTTGTACTCCTCCCTT GTC-3', 5'-GTAGCACCCAGGAAACTAGCATTTATCTTT GAGCTTGGGAGAGCTAGGGCAGGCAGATA AGGT-3' and R6 for -112 ~ -96, respectively. For constructing hNTCP promoter carrying these five mutations (5-Mut), five DNA segments were amplified using the primers as follows: for segment 1, F1 and 5'- GAGGGGATGTGTCCATGACC-3'; for segment 2, 5'-AGCTCCTTTCACTCTCATGGGT-3' and 5'-TCCTTTTCCCAGCTCCGC-3'; for segment 3, 5'-GAGCTGGGAAAAGGAGCTGC-3' and 5'-CCACTGAGTGTGCCTCATGG-3'; for segment 4, 5'- AGGCACACTCAGTGGAGGG-3' and 5'-CTGGGTGCTACTTGTACTCCTCC-3'; for segment 5, 5'-CAAGTAGCACCCAGGAATCCA-3' and R6. For producing a deletion construct for hNTCP promoter, phNTCP (-53~+108)-Gluc, DNA fragment was amplified using the primer sets 5'-GGTGAATTCTGTTCCTCTTTGGGGCGACAG C-3' and 5'-GGTGGTAAGCTTTCCTTGTTC TCCGGCTGACTCC-3' and then inserted into the EcoRI and HindIII sites of phNTCP-Gluc.

HBV preparation and infection

HBV was prepared and infected as described (19). HBV used in this study was mainly derived from HepAD38 cells (22). For Fig. 6A-E, we used concentrated (approximately 200-fold) media of HepG2 cells transfected with an expression plasmid for either HBV genotype A, B, C, D, or genotype C carrying mutations at L180M, S202G, and M204V [HBV/Aeus, HBV/Bj35s, HBV/C-AT, HBV/D-IND60, or HBV/C-AT(L180M/S202G/M204V)] (24), and infected into the cells at 2000 GEq/cell in the presence of 4% PEG8000 at 37 °C for 16 h as previously described (19). HBV for Fig. 6F (genotype C) was purchased from Phoenixbio.

Real time PCR and RT-PCR

Real time PCR for detecting HBV DNAs and cccDNA was performed as described (19). RT-PCR detection of mRNAs for NTCP, ASBT, SHP, and GAPDH was performed with one step RNA PCR kit (TaKaRa) following the manufacturer's protocol with primer set 5'-AGGGAGGAGGTGGCAATCAAGAGTGG-3' and 5'-CCGGCTGAAGAACATTGAGGCACTGG-3' for NTCP, 5'- GTTGGCCTTGGTGATGTTCT-3' and 5'- CGACCCAATAGGCCAAGATA-3' for ASBT, 5'- CAGCTATGTGCACCTCATCG-3' and 5'- CCAGAAGGACTCCAGACAGC-3' for SHP, and 5' -CCATGGAGAAGGCTGGGG-3' and 5'-CAAAGTTGTCATGGATGACC-3' for GAPDH, respectively.

Immunofluorescence analysis

Immunofluorescence was conducted essentially as described (25) using an anti-HBc antibody (DAKO, #B0586) at a dilution of 1:1,000.

Detection of HBs and HBe antigens

HBs and HBe antigens were detected by ELISA and chemiluminescence immunoassay, respectively, as described (19).

MTT assay

The MTT cell viability assay was performed as described previously (19).

Southern blot analysis

Isolation of cellular DNA and southern blot analysis to detect HBV DNAs were performed as described previously (19).

Immunoblot Analysis

Immunoblot analysis was performed as described previously (26,27). Anti-NTCP (Abcam) (1:2000 dilution), anti-RARα (Santa Cruz Biotechnology) (1:6000 dilution), anti-RARβ (sigma) (1:6000 dilution), anti-RARγ (abcam) (1:2000 dilution), anti-RXRα (Santa Cruz Biotechnology) (1:8000 dilution), and anti-actin (Sigma) (1:5000 dilution) antibodies were used for primary antibodies.

Flow cytometry

Downloaded from http://www.jbc.org/ at National Institute of Infectious Diseases LIBRARY on February 13, 2015

1 x 10^6 primary human hepatocytes were incubated for 30 min with a 1:50 dilution of anti-NTCP Ab (Abcam), then washed and incubated with a dye-labeled secondary Ab (Alexa Fluor 488, Invitrogen) at 1:500 dilution in the dark. Staining and washing were carried out at 4 °C in PBS supplemented with 0.5% bovine serum albumin and 0.1% sodium azide. The signals were analyzed with Cell Sorter SH8000 (SONY).

FITC-preS1 peptide-binding assay

Attachment of preS1 peptide with host cells was examined by preS1-binding assay essentially as described previously (28). HepaRG cells treated with or without Ro41-5253 (28) for 24 h or unlabeled preS1 peptide for 30 min were incubated with 40 nM FITC-labeled preS1 peptide (FITC-preS1) at 37°C for 30 min. After washing the cells twice with culture medium and once with phosphate-buffer saline (PBS), the cells were fixed with 4% paraformaldehyde. Then, the cells were treated with 4% Block Ace (DS Pharma Biomedical) containing DAPI for 30 min.

Reporter assay

HuS-E/2 cells were transfected with phNTCP-Gluc (GeneCopoeia), a reporter plasmid carrying the NTCP promoter sequence upstream of the Gaussia luciferase (Gluc) gene, and pSEAP (GeneCopoeia), expressing the secreted alkaline phosphatase (SEAP) gene, together with or without expression plasmids for RARα, RARβ, RARγ with RXRα using lipofectamine 2000 (Invitrogen). At 24 h posttransfection, cells were stimulated with the indicated compounds for further 24 h. The activities for Gluc as well as for SEAP were measured using a Secrete-Pair Dual Luminescence Assay Kit (GeneCopoeia) according to the manufacturer's protocol, and Gluc values normalized by SEAP are shown.

pRARE-Fluc, carrying three tandem repeats of RAR binding elements upstream of Firefly luciferase (Fluc) and pTK-Rluc (Promega), which carries herpes simplex virus thymidine kinase promoter expressing Renilla luciferase (Rluc) (25), were used in dual luciferase assays for detecting Fluc and Rluc. Fluc and Rluc were measured with Dual-Luciferase Reporter Assay System (Promega) according to the manufacture's protocol, and Fluc activities normalized by Rluc are shown.

For evaluating HBV transcription in Fig. 2B, we used a reporter construct carrying HBV enhancer I, II, and core promoter (nt 1039-1788) ("Enh I+II"), that carrying enhancer II and core promoter (nt 1413-1788) ("Enh II") that are derived from a genotype D HBV in HepG2.2.15 cells, which was inserted into pGL4.28 vector (Promega), and pGL3 promoter vector (Promega), which carries SV40 promoter ("SV40") as a control.

Chromatin immunoprecipitation (ChIP) assay

ChIP assay was performed using a Pierce Agarose ChIP Kit (Thermo Fisher Scientific) according to the manufacturer's instructions. Huh7-25 cells transfected with phNTCP-Gluc together with or without expression plasmids for FLAG-tagged RARα and for RXRα were treated with 5 μg/ml actinomycin D for 2 h. The cells were then washed and treated with or without 2 μM ATRA for 60 min. Formaldehyde cross-linked cells were lyzed, digested with micrococcal nuclease, immunoprecipitated with anti-FLAG antibody (Sigma) or normal IgG. Input samples were also recovered without immunoprecipitation. DNA recovered from the immunoprecipitated or the input samples was amplified with primers 5'-CCCAGGGCCCACCTGAATCTA-3' and 5'-TAGATTCAGGTGGGCCCTGGG-3' for detection of NTCP.

Results

Anti-HBV activity of Ro41-5253

We searched for small molecules capable of decreasing HBV infection in a cell-based chemical screening method using HBV-susceptible HepaRG cells (29). As a chemical library, we used a set of compounds of which bioactivity is already characterized (19). HepaRG cells were pretreated with compounds and then further incubated with HBV inoculum in the presence of compounds for 16 h (Fig. 1A). After removing free HBV and compounds by washing, the cells were cultured for an additional 12 days without compounds. For robust screening, HBV infection was monitored by ELISA quantification of HBs antigen secreted from the infected cells at 12 days postinfection. This screening revealed that HBs was significantly reduced by treatment with Ro41-5253 (Fig. 1B) as well as heparin, a competitive viral attachment

Downloaded from http://www.jbc.org/ at National Institute of Infectious Diseases LIBRARY on February 13, 2015

inhibitor which served as a positive control (14) (Fig. 1C). HBe in the medium (Fig. 1D) as well as intracellular HBc protein (Fig. 1F), HBV replicative (Fig. 1G), and cccDNA (Fig. 1H) were consistently decreased by treatment with Ro41-5253, without serious cytotoxicity (Fig. 1E). This effect of Ro41-5253 was not limited to infection of HepaRG cells because we observed a similar anti-HBV effect in primary human hepatocytes (Fig. 1I). The anti-HBV effect of Ro41-5253 on HBV infection of primary human hepatocytes was also observed in the absence of PEG8000 (Fig. 1J), which is frequently used to enhance HBV infectivity *in vitro* (14,29). These data suggest that Ro41-5253 treatment decreases hepatocyte susceptibility to HBV infection.

Reduced HBV entry in Ro41-5253-treated cells

Ro41-5253 decreased HBs secretion from infected cells in a dose-dependent manner without significant cytotoxicity (Fig. 2A). We next investigated which step in the HBV life cycle was blocked by Ro41-5253. The HBV life cycle can be divided into two phases: 1) the early phase of infection including attachment, internalization, nuclear import, and cccDNA formation, and 2) the following late phase representing HBV replication that includes transcription, pregenomic RNA encapsidation, reverse transcription, envelopment, and virus release (19,20,30-34). LMV and ETV, inhibitors of reverse transcriptase, dramatically decreased HBV DNA in HepAD38 cells (Fig. 2B, left), which can replicate HBV DNA but are resistant to infection (22). However, LMV and ETV did not show a significant effect in HepaRG-based infection (Fig. 1A), in contrast to the anti-HBV effect of CsA, an HBV entry inhibitor (19,35) (Fig. 2C), suggesting that this infection assay could be used to evaluate the early phase of infection without the replication process including the reverse transcription. Ro41-5253 was suggested to inhibit the early phase of infection prior to genome replication as an anti-HBV activity was evident in Fig. 2C but not in Fig. 2B. Moreover, Ro41-5253 had little effect on HBV transcription, which was monitored by a luciferase activity driven from the HBV enhancer I, II, and the core promoter (Fig. 2B, middle), and by the HBV RNA level in HepG2.2.15 cells, persistently producing HBV (36) (Fig. 2B, right). We then examined whether Ro41-5253 pretreatment affected viral attachment to host cells. To this end, HepaRG cells were exposed to HBV at 4℃ for 3 h, which allowed HBV attachment but not subsequent internalization (19) (Fig. 2D). After washing out free viruses, cell surface HBV DNA was extracted and quantified to evaluate HBV-cell attachment (Fig. 2D). Pretreatment with Ro41-5253 significantly reduced HBV DNA attached to the cell surface, as did heparin (Fig. 2D). In a preS1-binding assay, where FITC-labeled preS1 lipopeptide was used as a marker for HBV attachment to the cell surface, Ro41-5253-treated cells showed a reduced FITC fluorescence measuring viral attachment (Fig. 2E). Thus, Ro41-5253 primarily decreased the entry step, especially viral attachment. Next, to examine whether Ro41-5253 targeted HBV particles or host cells, HepaRG cells pretreated with compounds were examined for susceptibility to HBV infection in the absence of compounds (Fig. 2F). As a positive control, HBV infection was blocked by pretreatment of cells with an NTCP-binding lipopeptide, preS1(2-48)^{myr} (preS1 peptide) (15), but not by heparin, which binds HBV particles instead (14) (Fig. 2F, lanes 2 and 3). HBV infection was also diminished in HepaRG cells pretreated with IL-1β, which induced an innate immune response (37) (Fig. 2F, lane 4). In this experiment, Ro41-5253-pretreated HepaRG cells were less susceptible to HBV infection (Fig. 2F, lane 5), suggesting that the activity of Ro41-5253 in host cells contributed to the inhibition of HBV entry.

Ro41-5253 downregulated NTCP

Next, we examined how treatment of hepatocytes with Ro41-5253 decreased HBV susceptibility. Recently, NTCP was reported to be essential for HBV entry (15). Intriguingly, we found that Ro41-5253 decreased the level of NTCP protein in HepaRG cells (Fig. 3A). Flow cytometry showed that NTCP protein on the cell surface was consistently downregulated following treatment with Ro41-5253 (Fig. 3B, compare red and blue). Semi-quantitative RT-PCR revealed that mRNA levels for NTCP, but not apical sodium-dependent bile salt transporter (ASBT, also known as NTCP2 or SLC10A2), another SLC10 family transporter, were reduced by Ro41-5253 in HepaRG cells (Fig. 3C). Thus, Ro41-5253 could reduce NTCP expression. When endogenous NTCP and RAR

Downloaded from http://www.jbc.org/ at National Institute of Infectious Diseases LIBRARY on February 13, 2015

was knocked down by siRNA, the anti-HBV effect of Ro41-5253 was significantly diminished (Fig. 3D), suggesting that the inhibitory activity of Ro41-5253 to HBV infection was, at least in part, mediated by targeting NTCP. These data suggest that Ro41-5253 downregulated NTCP, which probably contributed to the anti-HBV activity of Ro41-5253.

Retinoic acid receptor regulated NTCP promoter activity

To determine the mechanism for Ro41-5253-induced downregulation of NTCP, we used a reporter construct inserting nucleotides (nt) -1143 ~ +108 of the human NTCP (hNTCP) promoter upstream of the Gluc gene (Fig. 4A, upper). Ro41-5253 dose-dependently decreased the luciferase activity driven from this promoter, although the effect was modest that showed up to approximately 40% reduction (Fig. 4A, left). Ro41-5253 had little effect on the herpes simplex virus thymidine kinase promoter (Fig. 4A, right), suggesting that Ro41-5253 specifically repressed hNTCP promoter activity. As reported previously (38), Ro41-5253 specifically inhibited retinoic acid receptor (RAR)-mediated transcription (Fig. 4B, C). RARα, RARβ, and RARγ are members of the nuclear hormone receptor superfamily, which are ligand-activated transcription factors that regulate the transcription of specific downstream genes by binding to RAR responsive element (RARE) predominantly in the form of heterodimer with retinoid X receptor (RXR). We therefore asked whether RAR could regulate the hNTCP promoter. As shown in Fig. 4D, hNTCP promoter activity was stimulated by overexpression of either RARα, RARβ, or RARγ together with RXRα, and transcription augmented by RAR could be repressed by Ro41-5253 (Fig. 4D). Knockdown of endogenous RARα, RXRα, or both dramatically impaired the activity of the hNTCP promoter (Fig. 4E). These results suggest that RAR/RXR is involved in the transcriptional regulation of the hNTCP gene. Consistently, an RAR agonist, ATRA, induced NTCP mRNA expression (Fig. 4F).

Importantly, endogenous expression of RARα was more abundant in differentiated HepaRG cells which are susceptible to HBV infection, than that in undifferentiated HepaRG and HepG2 cells, which are not susceptible (29) (Fig. 4G). This expression pattern was consistent with the expression of NTCP and with HBV susceptibility, suggesting the significance of RAR in regulating NTCP expression.

Promoter analysis of hNTCP

We next examined whether RAR regulation of hNTCP promoter is direct or indirect. From the analyses so far using rat Ntcp (rNtcp) promoter, one of the major regulators for rNtcp expression is farnesoid X receptor (FXR), which is a nuclear receptor recognizing bile acids (39). FXR, which is activated upon intracellular bile acids, indirectly regulates rNtcp expression: FXR induces its downstream small heterodimer partner (Shp), another nuclear receptor, and Shp recruits to rNtcp promoter to repress the promoter activity (39). Then, we examined whether RAR affected the expression of human SHP. As shown in Fig. 5A, while a FXR agonist GW4064 remarkably induced SHP expression as reported (39), RAR did not have a remarkable effect on SHP level in HepaRG cells (Fig. 5A). To assess the direct involvement of RAR in hNTCP regulation, ChIP assay showed that RAR was associated with hNTCP promoter both in the presence and absence of ATRA (Fig. 5B), consistent with the characteristic that RAR/RXR binds to RARE regardless of ligand stimulation (40). The genomatix software predicts that hNTCP promoter possesses five putative RAREs in nt -1143 ~ +108 (Fig. 5C). Introduction of mutations in all of these five elements lost the promoter activation by RAR/RXR overexpression (Fig. 5C, "5-Mut"). While the promoters mutated in the motif nt -491~-479, -368~-356, -274~-258, or -179~-167 was activated by ectopic expression of RAR/RXR and this activation was cancelled by Ro41-5253 treatment, the hNTCP promoter with mutations in nt -112~-96 had no significant response by RAR/RXR (Fig. 5C). These data suggest that the nt -112 to -96 region is responsible for RAR-mediated transcriptional activation of hNTCP.

HBV susceptibility was decreased in RAR-inactivated cells

We further investigated the impact of RAR antagonization on HBV infectivity. BMS195614, BMS493, and MM11253, which repressed RAR-mediated transcription (Fig. 6A), all decreased the susceptibility of HepaRG cells to HBV infection

Downloaded from http://www.jbc.org/ at National Institute of Infectious Diseases LIBRARY on February 13, 2015